FORMATION OF HYDROGELS FROM ANTIOXIDATIVE SYNTHETIC HYDROXYCINNAMATE ESTER CONJUGATES BASED ON CORN BRAN ARABINOXYLAN

YANLI LI

College of Chemistry and Engineering, Sichuan University of Science and Engineering, 519, Huixing Road, Ziliujing District, Zigong 643000, China
✉ *Corresponding author: liyanli0523@suse.edu.cn*

Received March 2, 2022

Corn bran arabinoxylan (CAX) was extracted from corn bran and modified through conjugating to four hydroxycinnamic acids (HAs), namely ferulic acid (FA), *p*-coumaric acid (*p*-CA), caffeic acid (CA), and sinapic acid (SA). These HA arabinoxylan esters (HA-CAX-*n*) exhibited analogous *n*-degrees of substitution (DS), FA-CAX-0.31, *p*-CA-CAX-0.32, CA-CAX-0.32, and SA-CAX-0.31. The antioxidant capacity was evaluated by a chemical method – an oxygen radical antioxidant capacity (ORAC) assay – and cellular models – a cellular antioxidant activity (CAA) assay to healthy human skin fibroblasts (HSF). The results of the various analyses were comparable, demonstrating the order of antioxidant capability was: CA-CAX-0.32 > SA-CAX-0.31 > FA-CAX-0.31 > p-CA-CAX-0.32. HA-CAX-n gels with different crosslinking ability were obtained with the concentration of 0.5% (w/v) during oxidative gelation by laccase, SA-CAX-0.31 can form gels most easily, followed by FA-CAX-0.31, CA-CAX-0.32 and p-CA-CAX-0.32.

Keywords: arabinoxylan, modification, antioxidant, gel, hydroxycinnamic acid

INTRODUCTION

Polysaccharides are widely distributed in animals, plants, and microorganisms. They possess a variety of biological activities, including antitumor, antiviral, heparinoid and immune modulation effects.[1,2] In recent years, polysaccharides from edible and medicinal plants have provoked interest as potential sources of novel antioxidants.[3]

Arabinoxylan (AX) represents the major hemicellulose structures of cereals. AX plays a critical role in maintaining the structural integrity of the cell walls in wheat, rice, barley, rye, oat, sorghum species *etc*.[4] The structure of arabinoxylan is very complex, but the primary chain consists of a linear backbone of α-(1-4)-linked β-D-xylopyranose residues to which α-L-arabinofuranose units are attached through O-2 and/or O-3, and some of the arabinofuranosyl residues are ester linked on (O)-5 by phenolic acids, such as ferulic acid (FA) and p-coumaric acid (p-CA).[5] The presence of hydroxycinnamic acids, such as p-coumaric, ferulic acid and its oligomers, provides biological activity to AX. AX and arabinoxylan oligosaccharides can act as prebiotics in the food and feed industry.[6] AX has gained interest as prebiotics for the probiotic bacteria, such as lactobacilli and bifidobacteria, in the large intestine.[7] It has been demonstrated that AX is associated with beneficial health effects in patients with impaired glucose tolerance and has potential as immuno-enhancing and antioxidant additive in functional foods.[8,9] More interestingly, it has been proved that the antioxidant activities of feruloyl oligosaccharides (FOs) were stronger than that of a free ferulic acid in a low-density lipoprotein oxidation system and a microsomal lipid peroxidation system, and bound ferulic acid from wheat bran was more bioavailable than the free ferulic acid.[10,11]

In addition to ferulic acid and *p*-coumaric acid (*p*-CA), other hydroxycinnamic acids, such as caffeic acid (CA) and sinapic acid (SA), are also widely distributed in plant tissue. The free HAs display anti-inflammatory, anticancer, antioxidant and antimicrobial activity.[12] The structures of HAs (shown in Fig. 1) reveal that hydroxyl functions bound to the aromatic ring are unstable, therefore mainly bound to cell wall polysaccharides as esters.[13,14] Furthermore, AX could form highly viscous solution and gels with the presence of enzymatic free radical generating agents by oxidative crosslinking reactions, which have been performed in various oxidative enzymatic systems, mainly laccase/O_2 and peroxidase/H_2O_2.[15-17]

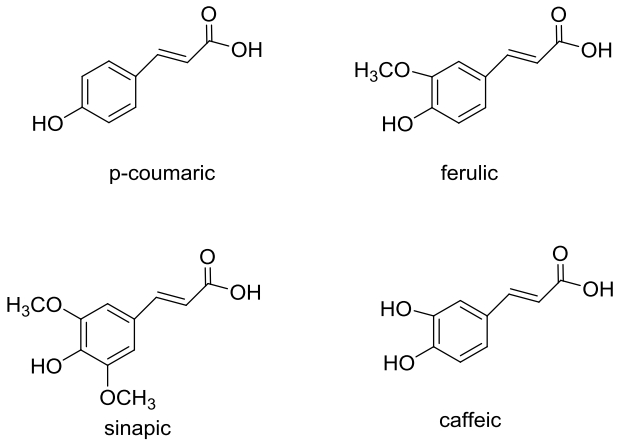

Figure 1: Structures of hydroxycinnamic acids investigated in this work

AXs, which are ester-linked to the cellulose, lignin, protein of bran, so AXs are usually extracted by alkaline aqueous solution, however phenolic acids can be hydrolyzed from AX, thereby the biological activity of AXs would be weakened.[18] The aim of this study was to mimic the naturally occurring arabinoxylans by attaching more HAs (including FA, p-CA, SA, CA) to CAX by esterification to produce HA-CAX-n (HA-CAX-n, n representing the degree of substitution) with more HA, and assess the antioxidant ability of CAX and HA-CAX-n with similar substitutive degrees on CAA and their cytotoxicity towards human skin fibroblasts (HSF), and the oxidative crosslinking ability of these modified CAXs. Polysaccharides maybe used to prepare antioxidant gels, providing broad application prospects.

EXPERIMENTAL

Materials

Ferulic acid (FA), p-coumaric acid (p-CA), sinapic acid (SA), caffeic acid (CA), deutero rifluoroacetic acid, deuterium oxide and thionylchloride were provided by Adamas (China). Trolox (6-hydroxy-2,5,7,8-tetramethylchroman-2-carboxylicacid), which is a hydrophilic analogue of vitamin E, 2,2'-azobis(2-amidinopropane) dihydrochloride (AAPH, also abbreviated ABAP), fluorescein sodium salt, 2',7'-dichlorofluorescin diacetate (DCFH-DA) and laccase were purchased from Sigma-Aldrich, Inc. (St. Louis, USA). Healthy human skin fibroblasts (HSF) were purchased from BeiNa Culture Collection (Beijing, China). Fetal bovine serum (FBS) was purchased from Gibco Life Technologies (Grand Island, NY). Phosphate-buffered saline (PBS), Dulbecco's modified Eagle's medium (DMEM) and Trypsin-EDTA were obtained from Hyclone (Logan, UT). Cell Counting Kit-8 (CCK-8) was purchased from Dojindo (Japan). Radio Immunoprecipitation Assay (RIPA) Lysis Buffer was bought from Beyotime Biotechnology Institute (Shanghai, China). All chemicals were of the highest purity commercially available.

Methods

Arabinoxylan extraction from corn bran

Corn bran was defatted, destarched and deproteinized by hexane, α-amylase and proteinase in turn. The residue (100 g) was suspended in 1 L of 1 M sodium hydroxide solution, 15 mL 30% H_2O_2 was added and incubated for 4 h at 60 °C. The suspension was cooled down at room temperature and centrifuged, the supernatant pH was adjusted to 6-7 using 1 M hydrochloric acid. Corn bran arabinoxylan (CAX) was precipitated from the supernatant with 4 volumes of absolute ethanol, the precipitate was freeze-dried. The method of extraction has been described in previous work.[19]

Synthesis of HA-CAX

Two parts of thionyl chloride ($SOCl_2$) were added slowly to one part of suspension of hydroxycinnamic acids (HA) in dichloromethane and the mixture was refluxed for 4 h under nitrogen. The resulting clear solution was distilled to remove solvent and excess $SOCl_2$, yielding HA chlorides, which were used without further purification.

CAX (1 g) in 30 mL DMA with LiCl (4%, w/w) was heated to 120 °C, while stirring until completely dissolved (~2 h). After cooling to room temperature, trithylamine (equivalent to ×1.5 the HA chlorides) was added and the prepared HA chlorides in DMA (5%, w/w) were added dropwise under nitrogen. Reaction mixtures including the HA chlorides of ferulic acid (FA), *p*-coumaric acid (*p*-CA), sinapic acid (SA), and caffeic

acid (CA) were stirred for 14, 12, 10 and 12 h, respectively, at 80 °C. After cooling to room temperature, four volumes of ethanol were added to precipitate the product. The precipitate was collected by centrifugation, washed three times with ethanol and freeze dried.

Molecular weight analysis

A Waters 600 high performance liquid chromatography (HPLC) system (Waters Co., USA), coupled to a refractive index detector, was used to determine the molecular weight of CAX and HA-CAX. Samples were dissolved in water (1 g/L) at room temperature and passed through 0.45 μm syringe filters before analysis. The HPLC mobile phase was 0.1 M aqueous sodium nitrate, the flow rate was 0.9 mL/min, and column temperature was 45 °C. Molecular weight was estimated by universal calibration with pullulan standard.

FT-IR spectroscopy

Fourier transform infrared (FT-IR) spectroscopy detects vibrations of chemical bonds and is used to identify functional groups. FT-IR spectra of CAX and HA-CAX (2 mg samples in 200 mg KBr pellets) were acquired using a Vector 22 FT-IR spectrometer (Bruker Co., Germany) operating at 4 cm^{-1} resolution.

^{1}H NMR and ^{13}C NMR spectroscopy

^{1}H and ^{13}C nuclear magnetic resonance (NMR) spectra were acquired using an AVANCE III HD 400 MHz spectrometer (Bruker, Germany), utilizing D_2O at 60 °C.

HA-CAX crosslinking and gel formation

Laccase (1.675 nkat/mg HA-CAX-n) as a crosslinking agent was added to HA-CAX-n solutions at 0.5% (w/v), respectively, and stirred evenly. The gels were allowed to develop at 25 °C for 2 h. Laccase was deactivated by boiling the samples for 10 min.

Hydroxycinnamic acids and di-hydroxycinnamic acids content of HA-CAX

The determination of hydroxycinnamic acid and di-hydroxycinnamic acid (DHA) content of HA-CAX followed a protocol previously described by Li.[6] Accordingly, HA-CAX was treated with 4% NaOH (1, 25, w/v) at 40 °C under ultrasonic waves for 30 min. The extracts were acidified with HCl to pH 3, extracted with ethyl acetate and filtered through a 0.22 μm nylon membrane. The HA and DHA released were determined by a Waters 1525μ High-Performance Liquid Chromatography (HPLC) system (Waters Co., USA). HPLC was performed using a C_{18} column (4.6 mm × 250 mm, 5 μm), monitored at 320 nm. The temperature of the column oven was set to 25 °C. The mobile phase was methanol-1% acetic acid (45:55), the flow rate was 1.0 mL/min and the injection volume was 20 μL. Detection was followed by UV absorbance at 320 nm.

The method of determining the degree of substitution (DS) was based on Li,[18] using the formula:

$$DS = \frac{M_H/W_H}{\frac{M}{W_X + W_A \times (A/X)}} \quad (1)$$

where M_H is the amount of released HA, W_H is the molecular weight of HA, M is the amount of HA-CAX, W_X is the molecular weight of the xylose unit, W_A is the molecular weight of the arabinose unit, and A/X is the ratio of arabinose to xylose.

Rheological properties

The rheological tests were monitored using a strain-controlled rheometer Discovery DHR-2 in oscillatory mode. The four types of HA-CAX-n were mixed with laccase. The dynamic rheological parameters were carried out at a frequency of 0.25 Hz and 1% strain.

ORAC determination

ORAC determination was based on the procedure described by Ou, Hampschwoodill and Prior.[20] An automated assay was carried out in 96-well plates using a Synergy 2 microplate reader (BioTek, USA) with fluorescence filters for 485 nm excitation wavelength and 535 nm emission wavelength. Peroxyl radicals were generated using 2,2'-azobis(2-amidino-propane) dihydrochloride (AAPH) freshly prepared for each run, Trolox was used as the standard, and fluorescein (FL) as the fluorescent probe.

In each well, 50 μL sample, blank (PBS), or standard (20 μM Trolox) was mixed with 50 μL FL (78 nM) and incubated for 15 min at 37 °C before addition of 25 μL AAPH solution (221 mM). The fluorescence was measured immediately and every 2 min until the relative fluorescence intensity was less than 5% of the initial reading. Stock solutions of FL, AAPH, Trolox and samples were prepared daily in phosphate buffered saline (PBS, 75 mM, pH 7.0).

ORAC values, expressed as μM Trolox equivalents (TE), were calculated as follows:

$$\text{ORAC } (\mu\text{M TE}) = \frac{C_{\text{Trolox}} \cdot (AUC_{\text{Sample}} - AUC_{\text{Blank}}) \cdot k}{AUC_{\text{Trolox}} - AUC_{\text{Blank}}} \quad (2)$$

where C_{Trolox} is the concentration of Trolox (20 µM), k is the sample dilution factor, and AUC is the area under the (fluorescence decay) curve determined from the formula:

$$AUC = 1 + f_1/f_0 + f_2/f_0 + f_3/f_0 + \ldots + f_i/f_0 \quad (3)$$

where f_0 is the initial fluorescence reading at 0 min and f_i is the fluorescence at time i.

Cell culture

Healthy human skin fibroblasts (HSF) were maintained in a 37 °C incubator (humidified atmosphere, 5% CO_2). Cells were cultured in DMEM supplemented with 10% FBS, 100 U/mL penicillin, and 100 µg/mL streptomycin. All experiments were carried out 24 h after cells were seeded at an appropriate density.

Cytotoxicity

Cytotoxicity toward HSF was measured using a commercial Cell Counting Kit-8 (CCK-8) employing WST-8 reagent (2-(2-methoxy-4-nitrophenyl)-3-(4-nitrophenyl)-5-(2,4-disulfophenyl)-2H-tetrazolium sodium salt) according to manufacturer's instructions. WST-8 is reduced to orange formazan by mitochondrial dehydrogenase. HSF were seeded at 10^4/well in a 96-well plate in 100 µL of growth medium and incubated for 24 h at 37 °C. The medium was then removed and 100 µL of medium containing various concentrations of CAX or HA-CAX were applied to the cells for 24 h. After various incubation times (37 °C, 5% CO_2), the medium was removed and replaced with WST-8 reagent in DMEM (10%, w/w). Cytotoxicity was determined by measuring the absorbance at 450 nm within 4 h using a GloMax 96 Microplate luminometer (Promega, USA). Cell viability (V_c) was calculated as follows:

$$V_c\ (\%) = \frac{A_s - A_b}{A_c - A_b} \times 100\% \quad (4)$$

where A_s is the absorbance of a sample, A_b the absorbance of a blank treated with WST-8 but without cells, and A_c – the absorbance of a control treated with cells and WST-8 but without antioxidant. Results are expressed as mean ± standard deviation of at least three replicates.

Cellular antioxidant activity of HA-CAX

The CAA assay protocol was adapted from Wolfe and Liu.[21] HSF were seeded into a 96-well black, clear-bottom microplate at a density of 5×10^4/well/100 µL growth medium and incubated for 24 h. Cells were then treated in triplicate for 1 h with 100 µL of medium containing HA-CAX with 25 µM DCFH-DA dye. The wells were washed with 100 µL PBS. 2,2'-Azobis(2-amidinopropane) dihydrochloride (ABAP, 600 µM) was then applied to the cells in 100 µL of DMEM and the microplate was analyzed using an Infinite M200 PRO plate reader at 37 °C (excitation at 485 nm, emission at 538 nm) every 5 min for 1 h. After blank subtraction from the fluorescence readings, the AUC of fluorescence versus time was integrated to give the CAA value as follows:

$$\text{CAA units} = 100 - (\int SA / \int CA) \times 100 \quad (5)$$

where ∫SA is the integrated area of the sample fluorescence versus time curve and ∫CA is the integrated area of the control curve.

RESULTS AND DISCUSSION

Preparation of HA-CAX-*n*

The optimized synthesis of CAX moderately esterified with hydroxycinnamic acids (*p*-CA, FA, SA, and CA) is shown in Figure 2. By controlling the reaction temperature and amount of $SOCl_2$, HA chlorides were prepared without protecting the hydroxyl groups. Percentage yields and DS are listed in Table 1. Native CAX contained a small amount of FA (DS of 0.023). HA-CAX-*n* represents HA-CAX with different (*n*) DS. The DS of HA-CAX was affected by the molar ratio of HA to anthydroxylose units (DS increased with increasing concentration of each HA) and all yields were above 90%.

HA-CAX-n with similar DS (namely, *p*-CA-CAX-0.32, FA-CAX-0.31, SA-CAX-0.31, and CA-CAX-0.32) were synthesized and subjected to comparative analysis. The M_w and polydispersity index (M_w/M_n) of each HA-CAX-n are given in Table 2. The M_w of native CAX was 3.06×10^5 g/mol. HA-CAX-n with similar DS exhibited similar M_w and polydispersity indices.

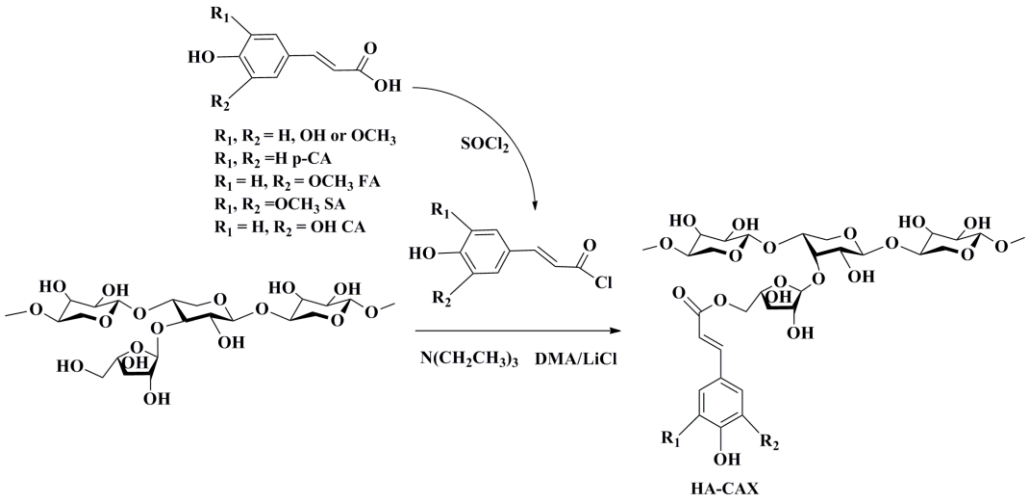

Figure 2: Synthesis of HA-CAX-n

Table 1
Yield and degree of substitution of HA-CAX-n

R	p-CA-CAX-n			SA-CAX-n			CA-CAX-n			FA-CAX-n		
	p-CA (mg/g)	DS	Yield (%)	SA (mg/g)	DS	Yield (%)	CA (mg/g)	DS	Yield (%)	FA (mg/g)	DS	Yield (%)
1, 5	18.32	0.28	92.4	18.77	0.21	90.7	19.39	0.27	90.2	23.99	0.31	93.6
1, 4	20.94	0.32	94.3	24.13	0.27	91.0	22.98	0.32	92.8	28.64	0.37	91.2
1, 3	24.21	0.37	93.6	27.70	0.31	91.9	31.59	0.44	92.5	30.96	0.40	92.5
1, 2	26.83	0.41	92.5	32.17	0.36	90.3	34.47	0.48	91.6	33.07	0.43	93.8
1, 1	28.14	0.43	90.9	34.89	0.39	92.1	35.19	0.49	91.3	34.83	0.45	92.7

Ratio, the molar ratio of each HA to anthydroxylose units

Table 2
Molecular weight of modified products HA-CAX

Samples	M_w(g/mol)	M_n(g/mol)	M_w/M_n
CAX	306539	95547	3.21
FA-CAX-0.31	351464	97041	3.62
p-CA-CAX-0.32	385042	98553	3.91
SA-CAX-0.31	370058	99465	3.72
CA-CAX-0.32	336296	93351	3.60

FT-IR spectroscopy of CAX and HA-CAX-n

FT-IR spectra of CAX and HA-CAX-n were acquired from 4000 to 400 cm^{-1} (Fig. 3). CAX exhibited broad absorbance across 1200-800 cm^{-1}, corresponding to the xylan backbone. The strong peak at 1042 cm^{-1} was ascribed to C-OH stretching in the pyranose ring. The peaks at 1191 cm^{-1} and 897 cm^{-1} were attributed to antisymmetric C–O–C stretching of the glycosidic link and the β-1,4-glycosidic bond. The broad absorbance across 3500-1800 cm^{-1} encompassed the "fingerprint" region of arabinoxylan. HA-CAX produced new peaks at 1763 cm^{-1} and 1535 cm^{-1} attributed to the conjugated carbonyl group arising from the esterification of arabinoxylan and the phenyl ring of HA.[22]

NMR spectroscopy of CAX and HA-CAX-n

Native CAX and HA-CAX-n were analyzed by ^{1}H NMR and ^{13}C NMR to characterize in detail the structural features of the esterified xylans. In the ^{1}H NMR spectrum of CAX (Fig. 4), the deuterium reagent was evident at δ 5.0 ppm. The peak at δ 2.0-4.8 ppm represented the anomeric protons of terminal arabinose units linked to the main chain xylose residues. The peaks in the regions δ 4.2-4.5 ppm and 3.5-4.1 ppm were attributed to anomeric carbons of α-L-arabinofuranose and β-D-xylopyranose, respectively. The peaks at δ 4.47, 4.41, and 4.28 ppm arose from the anomeric protons of Araf linked to, respectively, O-3, O-2, and O-1 of the same Xylp residue on the backbone.

The peak at δ 4.5 ppm may be attributed to a disaccharide side chain with the structure β-D-Xylp-(1-2)-α-L-Araf linked to O-3 of Xylp on the main chain. The peak with chemical shifts at δ 3.5-4 ppm could be ascribed to β-linked galactose. Those at δ 3.93, 3.81, 3.73, and 3.66 ppm corresponded to O-3, O-1, O-2 and O-4 of β-D-xylopyranose, respectively. The assignment of structures to the peaks between δ 2.4 and 3.5 ppm was more difficult because of the substituted arabinose units (multiunit branches or branched branches). The spectrum of HA-CAX (Fig. 4) revealed new signals at δ 6.5 and 7.2 ppm, attributable to the olefin on HA. A further set of new signals around δ 6.8 ppm could be assigned to the aromatic rings introduced by the HAs.

^{13}C NMR analysis confirmed these assignments (Fig. 5). The ^{13}C NMR spectrum of CAX revealed peaks at δ 50-100 ppm corresponding to the backbone, while the peaks in the region of δ 70-72 ppm were attributed to α-L-arabinofuranosyl residues linked to β-D-xylopyranose at O-2 and/or O-3. The peaks at δ 101, 72, 68, 76, and 57 ppm corresponded to the C-1, C-2, C-3, C-4 and C-5 carbons of α-L-Araf residues. The peaks at δ 96, 75.5, 66, 64 and 62 ppm originated from β-D-Xylp units at the C-1, C-2, C-3, C-4 and C-5 carbons.

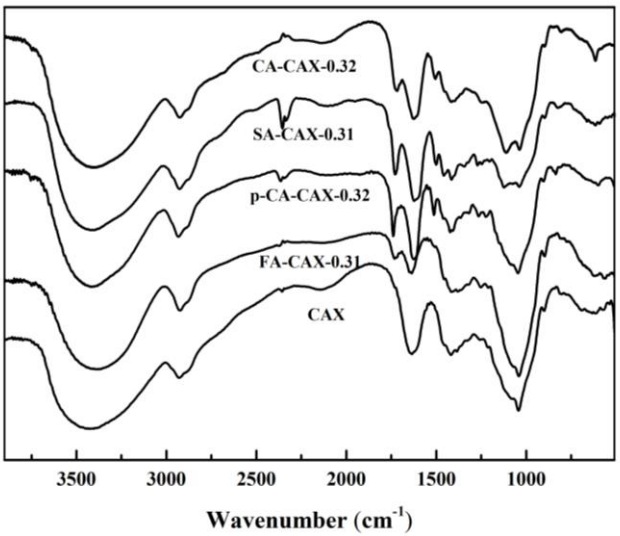

Figure 3: IR spectra of CAX and HA-CAX-n

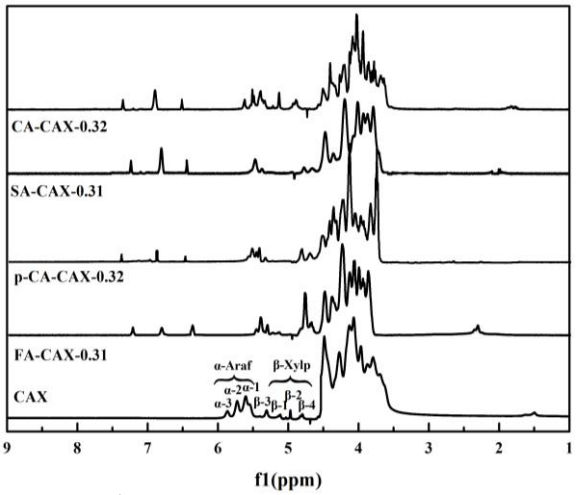

Figure 4: ^{1}H NMR spectra of CAX and HA-CAX-n

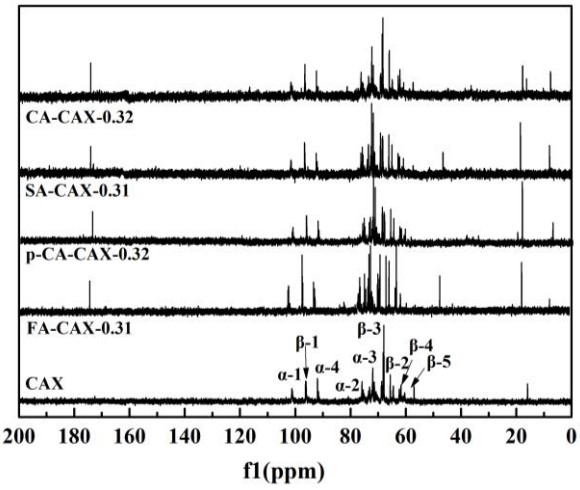

Figure 5: ^{13}C NMR spectra of CAX and HA-CAX-n

The ^{13}C NMR spectrum of HA-CAX showed the same signals for the xylan backbone and arabinofuranosyl as CAX, and all the HA-CAX spectra exhibited the ester bond at δ 174 ppm. The methoxy groups of FA-CAX-0.31 and SA-CAX-0.31 were identified by the signals at δ 46 ppm, where, due to the influence of the deuterated trifluoroacetic acid, they moved to the high field region.

Rheological properties and covalent crosslinks of HA-CAX-n gels

The formation of gel networks was monitored by storage (G') and loss (G") modulus changes in 0.5% (w/v) HA-CAX-n solutions undergoing oxidative gelation by laccase in Figure 6. The storage modulus G' is a measure of the energy that is stored in the material or recoverable per cycle of deformation, G" is a measure of the energy that is lost as viscous dissipation per cycle of deformation. As shown in Figure 6, the oxidative crosslinking kinetic profiles of HA-CAX-n demonstrated an initial increase of G', followed by plateaus, and exhibited solid-like behavior with G' > G". Thus, the increment of G' (*ΔG*') was used to evaluate the oxidative crosslinking ability. Obviously, the oxidative crosslinking ability of the four HA-CAX-n and CAX increased as follows: CAX < *p*-CA-CAX-0.32 < CA-CAX-0.32< FA-CAX-0.31 < SA-CAX-0.31. Laccase treatment of CAX and HA-CAX induced the crosslinking of arabinoxylan and produced strong gels, which is in agreement with the DHA content presented in Table 3.

Nevertheless, the tan δ (G"/G') values confirmed the formation of an elastic covalent system for both gels. Tan δ (G"/G') is used to indicate the evolution of gel strength: strong gel (<0.1), weak gel (0.1~1), or remaining solution (>1).[23] The 0.5% solutions of the HA-CAX-n formed strong gels with fast gelling speed (<2 min). SA-CAX-0.31 exhibited the strongest gels (tan δ = 0.01-0.08) successively, and *p*-CA-CAX-0.32, CA-CAX-0.32 and FA-CAX-0.31 formed weaker gels (tan δ = 0.07-0.9). However, in 0.5% solution, CAX performed the weakest gel (tan δ = 0.6). The behaviors in AX gels have been previously reported by several authors.[24-26] Similar rheological behaviors of AX treated above 4% have been observed;[27] after modification, HA-CAX formed gels treated with only 0.5%.

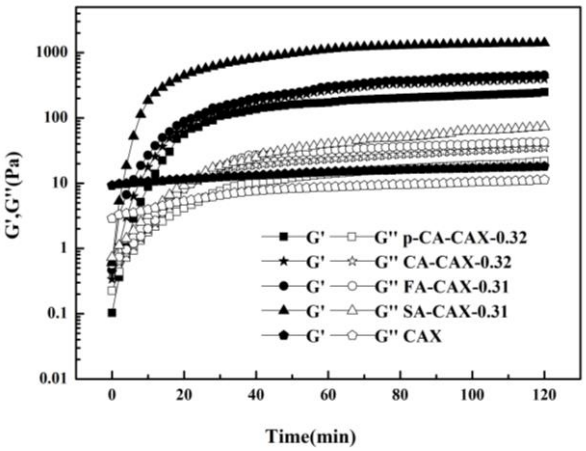

Figure 6: Monitoring the storage (G') and loss (G") moduli of HA-CAX-n solution at 1% (w/v) during gelation by laccase (1.675 nKat/mg of HA-CAX-n) at 0.25 Hz

Table 3
Dihydroxycinnamic acids (DHA) content in CAX and HA-CAX

Samples / Content (mg/g)	CAX	FA-CAX-0.31	p-CA-CAX-0.32	SA-CAX-0.31	CA-CAX-0.32
Diferulic acid	0.21	28.78	23.03	0.18	0.15
Dicoumaric acid	0.06	0.11	0.08	0.09	0.07
Disinapic acid	-	-	-	38.78	-
Dicaffeic acid	-	-	-	-	34.75
Total DHA	0.27	28.89	23.11	38.69	34.97

Hydroxycinnamoyl esters on the CAX molecules were supposed to be oxidized into radicals, forming crosslinks between CAX molecules. However, the four HA-CAX with similar DS show different oxidative crosslinking ability, SA-CAX > FA-CAX/CA-CAX > *p*-CA-CAX, which may have been related to the four HAs' structure. The SA with a hydroxyl and two methoxy groups has a more complex structure of side chains, FA and CA have two side chain groups, and p-CA has only one hydroxyl group. It should be mentioned that not only higher hydroxycinnamate crosslinking structures

to the participation of lignin residues coupled with HA monomers in the formation of gels, but also derivatization of hemicellulose hydroxyl groups may reduce the tendency of hemicelluloses to form strong hydrogen-bonded networks and increase film flexibility.

ORAC-fluorescein assay

The ORAC-fluorescein assay is a convenient method that has been widely employed for the estimation of the antioxidant capacity of pure compounds and complex mixtures. This assay measures the protection afforded by an antioxidant to a target molecule that is being oxidized by peroxyl radicals. This is the only method that combines the inhibition time and the percentage of free radical damage by the antioxidant into a single value, ensuring that, by the end of the process, all the antioxidants present in the sample have reacted with the radicals generated. The decrease in fluorescence intensity is monitored during the assay and a decay curve is constructed.

Figure 7 shows fluorescein fluorescence decay curves in the presence of Trolox, AAPH (blank), and various concentrations of the four HA-CAX. ORAC values were obtained from Equation (1) based on AUC, and corresponding concentrations are shown in Table 4. The blank control showed that, in the absence of an additive, a progressive decrease in fluorescence was observed over only 13 min. The addition of AAPH and CAX increased the fluorescence decay time to about 20 min. The addition of HA-CAX produced a lower rate of fluorescein consumption than CAX, with decay time being dose-dependent. Of the four HA-CAX studied, CA-CAX-0.32 produced the highest ORAC-fluorescein value (the slowest rate of fluorescein oxidation), followed by SA-CAX-0.31, FA-CAX-0.31 and *p*-CA-CAX-0.32, with native CAX yielding a value 1/3 to 1/2 of *p*-CA-CAX-0.32.

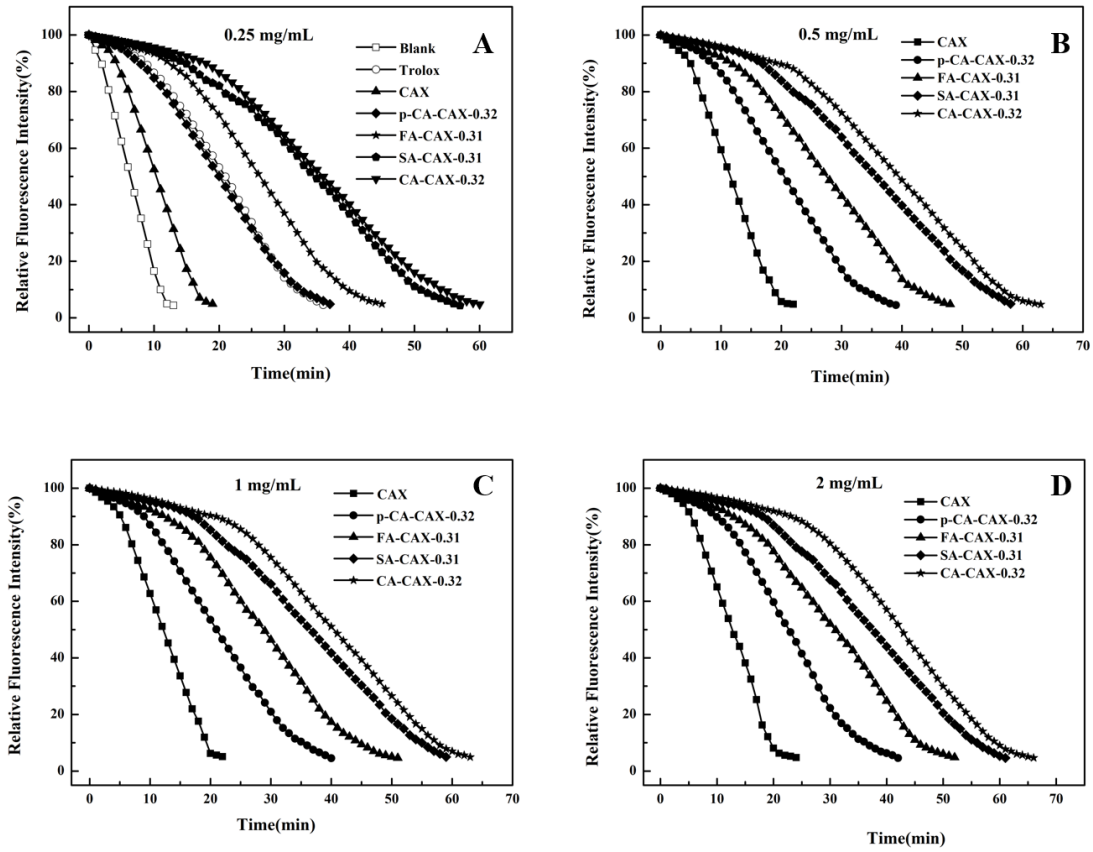

Figure 7: Fluorescence decay curves during the ORAC assay in the presence of various samples at different concentrations; A – CAX and HA-CAX treatment at 0.25 mg/mL, B – CAX and HA-CAX treatment at 0.5 mg/mL, C – CAX and HA-CAX treatment at 1 mg/mL, D – CAX and HA-CAX treatment at 2 mg/mL

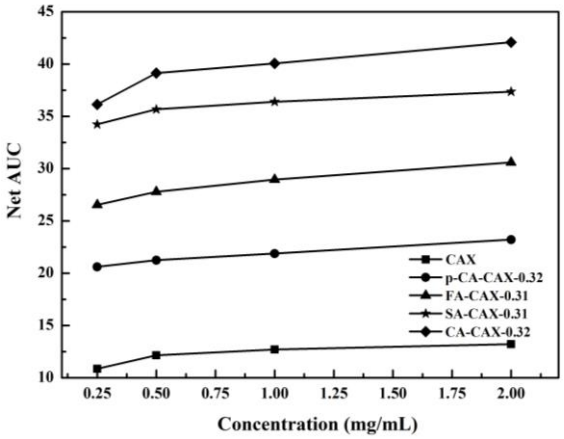

Figure 8: Regression of net AUC of CAX and HA-CAX-n at different concentrations (net AUC = $AUC_{sample} - AUC_{blank}$)

Table 4
Relative ORAC values of HA-CAX-n and CAX with antioxidant activity

Samples	ORAC			
	0.25 mg/mL	0.5 mg/mL	1.0 mg/mL	2.0 mg/mL
CAX	7.00	9.28	10.28	11.19
p-CA-CAX-0.32	28.24	29.07	32.06	35.05
FA-CAX-0.31	35.09	37.33	39.41	42.31
SA-CAX-0.31	48.83	51.38	52.69	54.41
CA-CAX-0.32	52.22	57.58	59.23	62.83

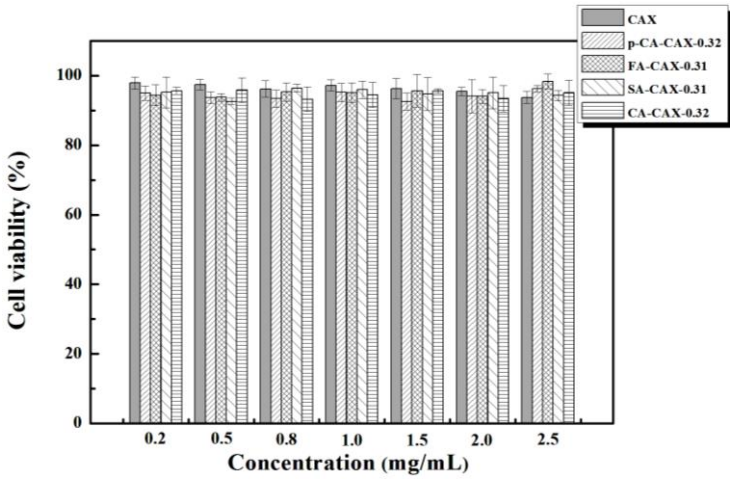

Figure 9: Cytotoxicity of CAX and HA-CAX-n at different concentration when incubated with HSF

For quantitation, net AUC (AUC_{Sample} - AUC_{Blank}) was calculated (Fig. 8). While net AUC for CAX and HA-CAX-n increased with increasing concentration, CAX was essentially inert in the ORAC assay. The increase in net AUC was dose-dependent in all cases, there was no lag phase, and fluorescence fell approximately exponentially from the start of the reaction.

Cytotoxicity

A fast and sensitive CCK-8 kit based on WST-8 reduction was used to assess cytotoxicity. The incubation of HSF with various concentrations of CAX and HA-CAX for 24 h affected less than 10% of the cells (Fig. 9). Neither CAX nor HA-CAX showed significant cytotoxicity toward HSF at the concentrations tested.

Cellular antioxidant activity assay

In the CAA assay, ABAP spontaneously decomposes to form peroxyl radicals, which induce the cell membrane to produce further radicals, which oxidize the DCFH-DA dye to fluorescent DCF following its cellular uptake. DCF fluorescence intensity represents the oxidation rate. Antioxidants can prevent the oxidation of membrane lipids and DCFH-DA, reducing DCF formation. This study is the first to use the CAA method to investigate the antioxidant potential of CAX and HA-CAX-n in HSF. Assay controls demonstrated the oxidation of ABAP over time in the absence of an oxidation inducer. CAX and HA-CAX-n inhibited oxidation, resulting in lower fluorescence than in controls (Fig. 10, a smaller area denotes higher CAA units and greater sample antioxidant activity). CA-CAX-0.32 exhibited the smallest area at each concentration, followed by SA-CAX-0.31, FA-CAX-0.31 and p-CA-CAX-0.32, each having significantly stronger antioxidant ability than CAX. Dose-dependent curves and median effect plots for CAX and HA-CAX are shown in Figure 11. CA-CAX-0.32 demonstrated significantly higher CAA than CAX and the other HA-CAX at the same concentration, the order being: CA-CAX-0.32 > SA-CAX-0.31 > FA-CAX-0.31 > *p*-CA-CAX-0.32 > CAX. ABAP-induced oxidation of DCFH in HSF and inhibition of this oxidation by CA-CAX-0.32 at 2 mg/mL is illustrated in Figure 12.

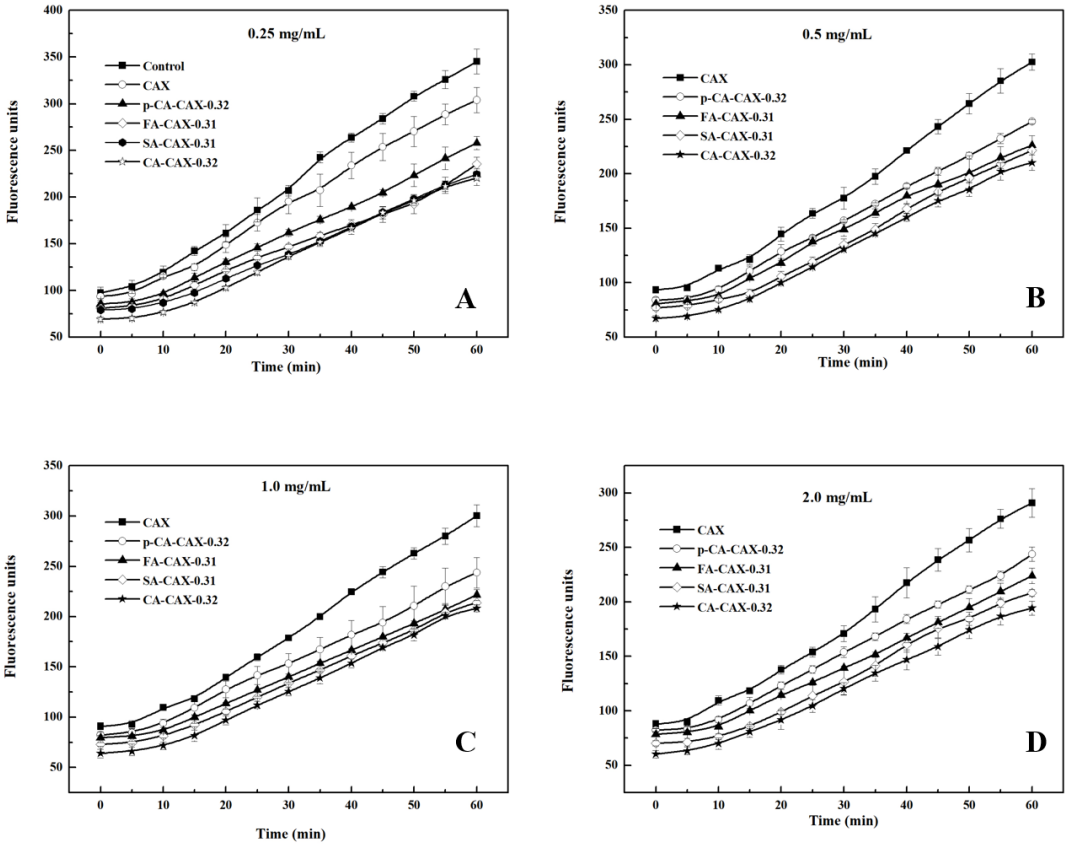

Figure 10: Peroxyl radical-induced oxidation of DCFH to DCF in HSF and the inhibition of oxidation by CAX and HA-CAX-n at different concentration; A – CAX and HA-CAX-n treatment at 0.25 mg/mL, B – CAX and HA-CAX-n treatment at 0.5 mg/mL, C – CAX and HA-CAX-n treatment at 1 mg/mL, D – CAX and HA-CAX-n treatment at 2 mg/mL

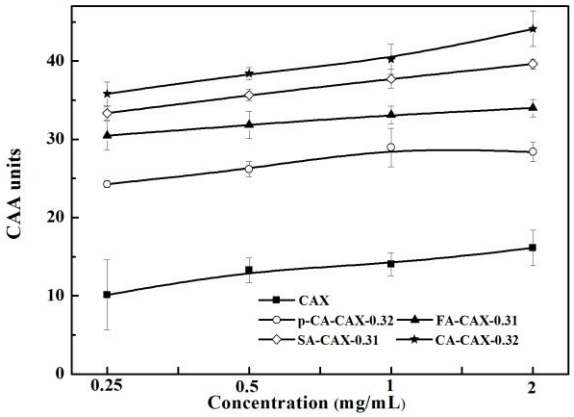

Figure 11: Dose-response curve for inhibition of oxidation of peroxyl radical-induced DCFH to DCF in HSF using the CAA assay in the presence of CAX and HA-CAX-n (the curves shown are each from a single experiment (mean ± SD, n = 3))

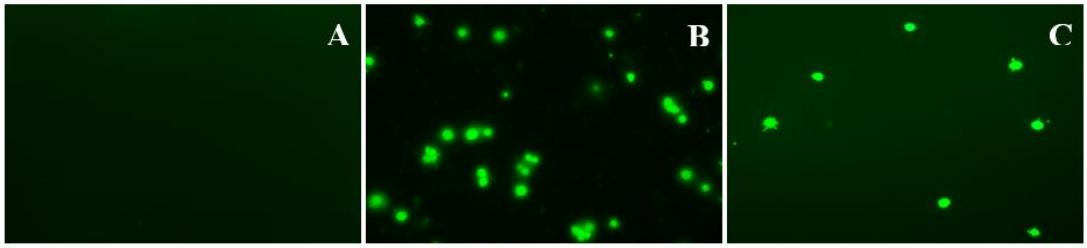

Figure 12: Micrographs of HSF taken by a fluorescence microscope; A – HSF without ABAP, B – HSF with ABAP, C – HSF with 2 mg/mL CA-CAX-0.32 and ABAP

HAs mediate their antioxidative effects by yielding hydrogen from their phenolic-OH groups to free radicals.[19] This structural relationship between phenolic acids and their antioxidant capacity is well established. The presence of the –CH=CH–COOR chain in HAs and their derivatives facilitates stabilization of the radical, initially by dehydrogenative oxidation of the phenolic hydroxyl, since the double bond participates in stabilizing the phenoxyl radical by resonance.[28] Antioxidative capacity is further influenced by electron-donating substituents. Phenolic compounds with one hydroxyl group on their aromatic ring are less effective antioxidants than those with a second hydroxyl in the ortho- or para- position. The antioxidative capacity of mono-phenols is also substantially increased by the presence of one or two methoxy substituents. Consequently, the antioxidant capability of the free HAs was the following: CA > SA > FA > *p*-CA. For HA-CAXs with similar DS, the antioxidant capability corresponded to that of the free HA. This study compared results from two cell-based models and a chemical assay applied to the same samples. Antioxidant activities were comparable across the two types of assay. The antioxidant capabilities of HA-CAX based on the ORAC and CAA assays were: CA-CAX-0.32 > SA-CAX-0.31 > FA-CAX-0.31 > *p*-CA-CAX-0.32. HA-CAX, which exhibited much stronger antioxidant capacity than CAX, is a promising natural material, which could potentially enhance the commercial value of corn bran. Human skin is constantly exposed to ultraviolet light and oxygen, leading to increased iron ion content. The topical administration of some of the substances evaluated in this study via semi-solid cosmetic or pharmaceutical formulations could afford protection to skin lipids. HAs, which are water insoluble and unstable antioxidants, linked to AXs as ester conjugates can hence function as strong water-soluble antioxidants, furthermore, can increased crosslinking of the AXs. HA-CAX is a promising and novel sunscreen additive, which could also be considered as a nutritional supplement in health care products and other application fields.[29,30]

CONCLUSION

In conclusion, hydroxycinnamic acid arabinoxylan esters (HA-CAX-n) with various degrees of substitution (DS) were synthesized and fully characterized. The properties of HA-CAX-n with similar DS were studied. All of them were well tolerated by the toxicity studies. Hydroxycinnamoyl groups esterified to CAX are considered to play a central role in antioxidant capacity and oxidative

crosslinking ability. Antioxidant capacity was detected by a chemical method – oxygen radical antioxidant capacity (ORAC) – and a cellular model – cellular antioxidant activity (CAA) assay – towards healthy human skin fibroblasts (HSF). The results of the two methods of HA-CAX-n were identical, the order of antioxidant activity was as follows: CA-CAX-0.32 > SA-CAX-0.31 > FA-CAX-0.31 > p-CA-CAX-0.32. Hence, the order of antioxidant activity of modified polysaccharides was CA-CAX > SA-CAX > FA-CAX > p-CA-CAX, which was correlated to the free HA and the antioxidant activity improved significantly. Moreover HA-CAX-n have already demonstrated increased gel formation, the oxidative crosslinking ability being SA-CAX-0.31 > FA-CAX-0.31 >CA-CAX-0.32 > *p*-CA-CAX-0.32.

ACKNOWLEDGEMENTS: This work was supported by Science and Technology Department of Sichuan Province (Grant Number, 2020YFG0422), Science and Technology Department of Zigong City (Grant Number, 2019YYJC19), Talent Introduction Funds of Sichuan University of Science and Engineering (Grant Number, 2018RCL02), Chemical Synthesis and Pollution Control Key Laboratory of Sichuan Province (Grant Number, CSPC202102).

REFERENCES

[1] K. Buksa, A. Nowotna, R. Ziobro and W. Praznik. *J. Cereal. Sci*., **60**, 368 (2014), https://doi.org/10.1016/j.jcs.2014.05.009
[2] E. Noaman, N. K. Badr El-Din, M. A. Bibars, A. A. Abou Mossallam, M. Ghoneum, *Cancer. Lett*., **268**, 348 (2008), https://doi.org/10.1016/j.canlet.2008.04.012
[3] M. Mendis and S. Simsek, *Food. Hydrocolloid*., **42**, 239 (2014), https://doi.org/10.1016/j.foodhyd.2013.07.022.
[4] L. F. Gilmullina, M. L. Ponomareva, S. N. Ponomarev and G. S. Mannapova, *Chem. Mater*., **1**, 27 (2021), https://doi.org/10.14258/jcprm.2021017713
[5] S. Jeroen, D. Emmie, J. A. Delcour and Ch. M. Courtin, *J. Agric. Food. Chem*., **61**, 10173 (2013), https://doi.org/10.1021/jf403160x
[6] Y. Li and C. Yang, *Int. J. Cos. Sci*., **38**, 238 (2015), https://doi.org/10.1111/ics.12281
[7] S. F. Reis and N. Abu-Ghannam, *LWT-Food. Sci. Technol*., **55**, 269 (2014), https://doi.org/10.1016/j.lwt.2013.09.004-77
[8] A. B. Samuelsen, A. Rieder, S. Grimmer, T. E. Michaelsen and S. H. Knutsen, *Int. J. Mol. Sci*., **12**, 570 (2011), https://doi.org/10.3390/ijms12010570
[9] A. L. Martínez-López, E. Carvajal-Millan, V. Micard, A. Rascón-Chu, F. Brown-Bojorquez *et al*., *Carbohyd. Polym*., **144**, 76 (2016), https://doi.org/10.1016/j.carbpol.2016.02.031
[10] L. Y. Lin, Y. X. Wang, T. Zhang, J.-F. Zhang, M. Pan *et al*., *Carbohyd. Polym*., **249**, 116813 (2020), https://doi.org/10.1016/j.carbpol.2020.116813
[11] H. Y. Qiao, J. P. Dahiya and H. L. Classen, *Poultry Sci*., **87**, 719 (2008), https://doi.org/10.3382/ps.2007-00357
[12] P. Kylli, P. Nousiainen, P. Biely and J. Sipil, *J. Agric. Food. Chem*., **56**, 4797 (2008), https://doi.org/10.1021/jf800317v
[13] F. E. Ayala-Soto, S. O. Serna-Saldívar, S. García-Lara and E. Pérez-Carrillo, *Food. Hydrocolloid*., **35**, 471 (2014), https://doi.org/10.1016/j.foodhyd.2013.07.004
[14] V. Coman and C. V. Dan, *J. Sci. Food. Agr*., **100**, 483 (2020), https://doi.org/10.1002/jsfa.10010
[15] E. Carvajal-Millan, B. Guigliarelli, V. Belle and X. Rouau, *Carbohyd. Polym*., **59**, 181 (2005), https://doi.org/10.1016/j.carbpol.2004.09.008.
[16] E. Carvajal-Millan, S. Guilbert, J. L. Doublier and V. Micard, *Food. Hydrocolloid*., **20**, 53 (2006), https://doi.org/10.1016/j.foodhyd.2005.02.011
[17] C. M. Berlanga-Reyes, C. M. Elizabeth and L. M. Jaim, *Molecules*, **14**, 1475 (2009), https://doi.org/10.3390/molecules14041474
[18] L. Yanli, H. Tong, L. Rong, L. Zhengzhe, Z. Yuanbo *et al*., *Int. J. Biol. Macromol*., **106**, 1279 (2018), https://doi.org/10.1016/j.ijbiomac.2017.08.137
[19] L. Yanli, Z. Yuanbo, L. Rong and Y. Cheng, *Int. J. Cos. Sci*., **39**, 402 (2017), https://doi.org/10.1111/ics.12389
[20] B. Ou, M. Hampschwoodill and R. L. Prior, *J. Agric. Food. Chem*., **49**, 4619 (2001), https://doi.org/10.1021/jf010586o
[21] K. L. Wolfe and R. H. Liu, *J. Agric. Food. Chem*., **55**, 8896 (2009), https://doi.org/10.1021/jf0715166
[22] P. Wrigstedt, P. Kylli, L. Pitkanen, P. Nousiainen, M. Tenkanen *et al*., *J. Agric. Food. Chem*., **58**, 6937 (2010), https://doi.org/10.1021/jf9043953

[23] S. Y. Choh, D. Cross and C. Wang, *Biomacromolecules*, **12**, 1126 (2011), https://doi.org/10.1021/bm101451k
[24] W. Dridi and N. Bordenave, *Carbohyd*. *Polym*., **274**, 118670 (2021), https://10.1016/j.carbpol.2021.118670
[25] A. B. Hernández-Espinoza, M. I. Piñón-Muñiz, A. Rascón-Chu, V. M. Santana-Rodríguez and E. Carvajal-Millan, *Molecules*, **17**, 2428 (2012), https://doi.org/10.1021/jf010586o
[26] S. J. Jong, S. C. Smedt, J. Meester, C. F. van Nostrum, J. J Kettenes-van den Bosch *et al*., *J*. *Control*. *Release*., **72**, 47 (2001), https://doi.org/10.1016/S0168-3659(01)00261-9
[27] D. Tainara, D. Alessandro, V. Alves, N. Bandarra, M. Moldao-Martins *et al*., *Food*. *Bioprocess Tech*., **11**, 536 (2018), https://doi.org/10.1007/s11947-017-2030-0
[28] Y. Liu, Y. Zhang, K. Lin, D.-X. Zhang, M. Tian *et al*., *Life Science*, **94**, 99 (2013), https://doi.org/10.1016/j.lfs.2013.10.024
[29] U. Thiyam, H. Stöckmann, T. Z. Felde and K. Schwarz, *Eur*. *J*. *Lipid*. *Sci*. *Tech*., **108**, 239 (2006), https://doi.org/10.1002/ejlt.200500292
[30] X. Zhang, T. Chen, J. Lim, F. Gu, F. Fang *et al*., *Food*. *Hydrocolloid*., **91**, 1 (2019), https://doi.org/10.1016/j.foodhyd.2019.01.032